Forschungsberichte des

Institutes für Fertigungstechnologie keramischer Bauteile (IFKB)
Herausgeber: o. Prof. Dr. rer. nat. Dr. h.c. mult. Rainer Gadow

Martin Plachetta

Prozesstechnik und Simulation des Hochgeschwindigkeits-suspensionsflammspritzens

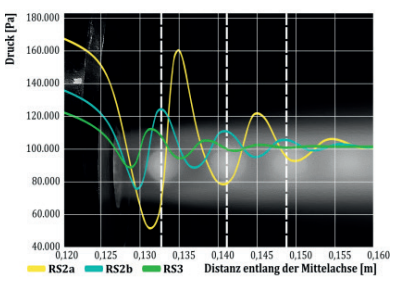

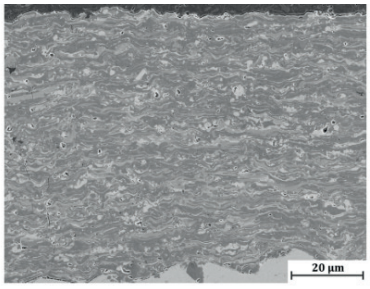

Universität Stuttgart

Graduate School of Excellence advanced Manufacturing Engineering in Stuttgart

Prozesstechnik und Simulation des Hochgeschwindigkeitssuspensionsflammspritzens

Von der Graduate School of excellence advanced Manufacturing Engineering
GSaME der Universität Stuttgart
zur Erlangung der Würde eines Doktor-Ingenieurs (Dr.-Ing.)
genehmigte Abhandlung

Vorgelegt von
Martin Plachetta
aus Bietigheim-Bissingen

Hauptberichter:
o. Prof. Dr. rer. nat. Dr. h.c. mult. Rainer Gadow
Mitberichter:
Prof. Dr. oec. publ. Wolfgang Burr
Prof. Dr. rer. nat. habil. Robert Vaßen

Tag der mündlichen Prüfung: 03.03.2020

Institut für Fertigungstechnologie keramischer Bauteile
der Universität Stuttgart
2020

Forschungsberichte des Instituts für
Fertigungstechnologie keramischer Bauteile (IFKB)

Martin Plachetta

Prozesstechnik und Simulation des Hochgeschwindigkeitssuspensionsflammspritzens

D 93 (Diss. Universität Stuttgart)

Shaker Verlag
Düren 2021

Bibliografische Information der Deutschen Nationalbibliothek
Die Deutsche Nationalbibliothek verzeichnet diese Publikation in der Deutschen Nationalbibliografie; detaillierte bibliografische Daten sind im Internet über http://dnb.d-nb.de abrufbar.

Zugl.: Stuttgart, Univ., Diss., 2020

ISBN 978-3-8440-7862-6
ISSN 1610-4803

Shaker Verlag GmbH • Am Langen Graben 15a • 52353 Düren
Telefon: 02421 / 99 0 11 - 0 • Telefax: 02421 / 99 0 11 - 9
Internet: www.shaker.de • E-Mail: info@shaker.de

Vorwort und Danksagung

Die vorliegende Arbeit entstand während meiner Tätigkeit am Institut für Fertigungstechnologie keramischer Bauteile (IFKB) und als Doktorand der Graduate School of Excellence advanced Manufacturing Engineering (GSaME) der Universität Stuttgart. Als Doktorand der GSaME wurde die Arbeit von der Deutschen Forschungsgemeinschaft (DFG) unterstützt.

Mein besonderer Dank gilt Herrn Prof. Dr. rer. nat. Rainer Gadow für seine wohlwollende Förderung und fachliche Unterstützung, die diese Arbeit möglich machten. Herrn Prof. Dr. oec. publ. Wolfgang Burr und Herrn Dr. rer. nat. habil. Robert Vaßen danke ich für das wissenschaftliche Interesse an dieser Arbeit und die Übernahme des Koreferats.

Herrn apl. Prof. Dr. rer. nat. Andreas Killinger danke ich für die konstruktive Zusammenarbeit und fachlichen Anregungen.

Ebenso danke ich den Mitarbeitern des IFKB, insbesondere meinen GSaME- und Zimmerkollegen sowie den Mitgliedern meiner IDA-Gruppe, für die gute Zusammenarbeit und gemeinsame Zeit, dabei besonders Herrn Dr. Venancio Martinez Garcia für seine fachliche und moralische Unterstützung, Herrn Dipl.Ing. Hans-Friedrich Jacobi für seine Beratung sowie den Studentinnen und Studenten, mit denen ich im Rahmen ihrer Studien- und Masterarbeiten zusammengearbeitet habe oder die als HiWi am Institut tätig waren.

Meinen Eltern danke ich für ihre Unterstützung über Studium und Promotionszeit hinweg.

Ein besonderer Dank geht an meine beste Freundin Katharina für ihre Geduld, Freundschaft und Unterstützung während der Anfertigung der Arbeit und meines gesamten Studiums.

Inhaltsverzeichnis

Abkürzungsverzeichnis

Abkürzung	Bedeutung
APS	Atmospärisches Plasmaspritzen
CFD	Numerische Strömungmechanik (engl. computational fluid dynamics)
CVD	chemische Gasphasenabscheidung (engl. chemical vapour deposition)
DC	Gleichstrom (engl. direct current)
EDM	Eddy-Dissipation-Modell
FSG	Feststoffgehalt der Suspension
gew.%	Gewichtsprozent
HVOF	Hochgeschwindigkeitsflammspritzen
HVPFS	Hochgeschwindigkeitspräkursorflammspritzen (engl. high velocity solution precursor flame spraying)
HVSFS	Hochgeschwindigkeitssuspensionsflammspritzen
IFKB	Institut für Fertigungstechnologie keramischer Bauteile
LDS	Lichtbogendrahtspritzen
LVE	Linear-viskoelastischer Bereich
PVD	Physikalische Gasphasenabscheidung (engl. physical vapour deposition)
REM	Rasterelektronenmikroskopie
Sl	Standardliter
SPS	Suspensionsplasmaspritzen (engl. suspension plasma spraying)
SPPS	Präkursorlösungsplasmaspritzen (engl. solution precursor plasma spraying)
SST	Shear-Stress-Transport-Modell
UV	Ultraviolett
XRD	Röntgendiffraktometrie (engl. x-ray diffraction)
YSZ	Durch Y_2O_3 stabilisiertes ZrO_2

Symbolverzeichnis

Symbol	Einheit	Bedeutung
A	$\frac{cm^{2,25}}{s*mol^{0,75}}$	Präexponentieller Faktor der Arrheniusgleichung
a	-	Koeffizient des EDM
A_{PS}	mm^2	Fläche des Prüfstempels
A_s	mm^2	Oberfläche der Vickerspyramide
b	-	Koeffizient des EDM
D	mm	Durchmesser der Düsenöffnung
Da	-	Damköhler-Zahl
$\mathrm{d_p}$	mm	Partikeldurchmesser
E_A	$\frac{kcal}{mol}$	Aktivierungsenergie
F_{max}	N	Maximale aufgewendete Kraft
G'	-	elastischer Schubmodul oder Speichermodul
G"	-	viskosen Schubmodul oder Verlustmodul
G*	-	komplexen Schubmodul
$\mathrm{h_C}$	$\frac{kJ}{g}$	Verbrennungsenthalpie
h_P	mm	Höhe der Vickerspyramide
$\mathrm{h_V}$	$\frac{kJ}{g}$	Verdampfungsenthalpie
HV	-	Härte Vickers
k	$\frac{m^2}{s^2}$	Turbulente kinetische Energie
L	mm	Durchmesser des Düsenzulaufs
l	mm	Charakteristische Länge
l_{BL}	mm	Dicke der Strömungs-Grenzschicht
m_B	g	Masse an eingesetztem Werkstoff
$\dot{m}$	$\frac{g}{min}$	Förderrate der Suspension
$\dot{m_g}$	$\frac{1}{s}$	Massenstrom der Gasphase
$\dot{m}_l$	$\frac{1}{s}$	Massenstrom der flüssigen Phase
n	-	Anzahl der Einzeltropfen
Oh	-	Ohnesorge-Zahl
Δp	Pa	Statische Druckdifferenz
r	mm	Tropfenradius
$r_{Düse}$	mm	Radius der Injektoröffnung
Rq	-	quadratischer Mittenrauwert (Linie)
Ra	µm	arithmetischer Mittenrauwert (Linie)
Re	-	Reynolds-Zahl
Rsk	-	Schiefe (Linie)

Rz	μm	gemittelte Rautiefe (Linie)
Sa	μm	arithmetischer Mittenrauwert (Fläche)
Sq	-	quadratischer Mittenrauwert (Fläche)
Ssk	-	Schiefe (Fläche)
St	-	Stokes-Zahl
Sz	μm	gemittelte Rautiefe (Fläche)
T_A	K	Aktivierungstemperatur
t_B	s	Beschichtungszeit
t_c	s	Chemische Zeitskala
t_p	s	Charakteristischen Zeit des Partikels
t_g	s	Charakteristischen Zeit einer umgebenden (Gas-) Strömung
t_t	s	Strömungsmechanische Zeitskala
T_V	$°C$	Verdampfungstemperatur
$\dot{V}$	$\frac{mm^3}{min}$	Den Injektor durchfließender Volumenstrom
v_f	-	Relativ-Geschwindigkeit des Fluids
v_{max}	$\frac{m}{s}$	Maximal erreichbare Geschwindigkeit des Fluids
ν_p	$\frac{m}{s}$	Partikelgeschwindigkeit
V_{ges}	mm^3	Gesamtes Flüssigkeitsvolumen
$\dot{V}_{real}$	$\frac{mm^3}{s}$	Realer Durchfluss
$\dot{V}_{theo}$	$\frac{mm^3}{s}$	Theoretischer Durchfluss
We	-	Weber-Zahl
$\dot{x}$	-	Massenstromverhältnis zwischen Gas und Flüssigkeit

Griechische Symbole

Symbol	Einheit	Bedeutung
β	-	Temperaturexponent
ε	$\frac{m^2}{s^3}$	Turbulente Dissipationsrate
$\dot{\gamma}$	$\frac{1}{s}$	Scherrate
ν	$\frac{m^2}{s}$	Kinematische Viskosität
η	$Pa * s$	Dynamische Viskosität
η_l	$Pa * s$	Dynamische Viskosität des Dispergiermediums
η_g	$Pa * s$	Dymanische Viskosität des Gases
μ	-	Durchflusszahl
ω	$\frac{1}{s}$	Spezifische turbulente Dissipationsrate
ϕ	-	Volumenanteil des Feststoffanteils
ρ	$\frac{kg}{m^3}$	Fluiddichte
ρ'	-	Dichteverhältnis
ρ_p	$\frac{kg}{m^3}$	Partikeldichte
σ	$\frac{N}{m}$	Oberflächenspannung
σ_H	$\frac{N}{mm^2}$	Haftzugfestigkeit
τ	$\frac{N}{mm^2}$	Schubspannung
τ_y	$\frac{N}{mm^2}$	Scherspannung
ν	$\frac{m}{s}$	Strömungsgeschwindigkeit des Fluids

Extended Abstract

Introduction For many applications, the relevant properties of a machine part are determined by its surface, like wear resistance, corrosion protection and thermal insulation. The application of a functional coating allows the optimisation of component volume and component surface independently of one another, offering benefits in design and economy. Thermal spraying has proven itself as a flexible and efficient group of processes that allow such coatings. The different thermal spraying processes available have a significant influence on the coating properties. Especially nano-sized particles delivered to the process by means of a suspension have been shown to result in coatings with extraordinary qualities, for example with regards to strength, hardness, ductility, and sinter activity. At the moment, the thermal spraying with suspensions finds few applications in the industry, available equipment is often in the status of prototypes. This stems partially from a lack of know-how about the differences in coating formation and a lack of process stability compared to conventional processes.

Central to the HVSFS process in particular is the internal, axial injection of the suspension into the combustion chamber of the spray torch. This way, the spray material is completely entrained in the flame, which leads to an enhanced transfer of momentum and heat compared to a radial injection of the particles. This internal injection however comes with higher demands towards the process stability since it places the injector outlet in the high temperature and pressure area of the combustion chamber. This can lead to a clogging of the injector nozzle due to untimely solvent evaporation and a build up of coating material inside the combustion chamber, which results in changed temperature and pressure conditions, negatively influencing process stability. Especially start-up and shut-down of the process are critical points.

This work aims to increase insight into influencing factors in the coating process with a focus on the torch components. The knowledge gained is used to develope the injector for the HVSFS process to be fit for industrial application.

In the first step, numerical simulation is used to determine critical temperature and pressure conditions that influence deposition of coating material inside the combustion chamber, particle melting behaviour and thermal strain on the injector components. Central point of the process is the injection of the suspension into the combustion chamber. Turbulent nozzles and newly developed two fluid nozzles are available for that. These will be compared experimentally to determine major influencing factors. To improve handling, the injector is to be redesigned in a modular concept that allows an adaption to process requirements by exchanging indiviual parts of the injector. Additionally, options for online process monitoring are to be implemented and their results will be compared with the results of the numerical simulation.

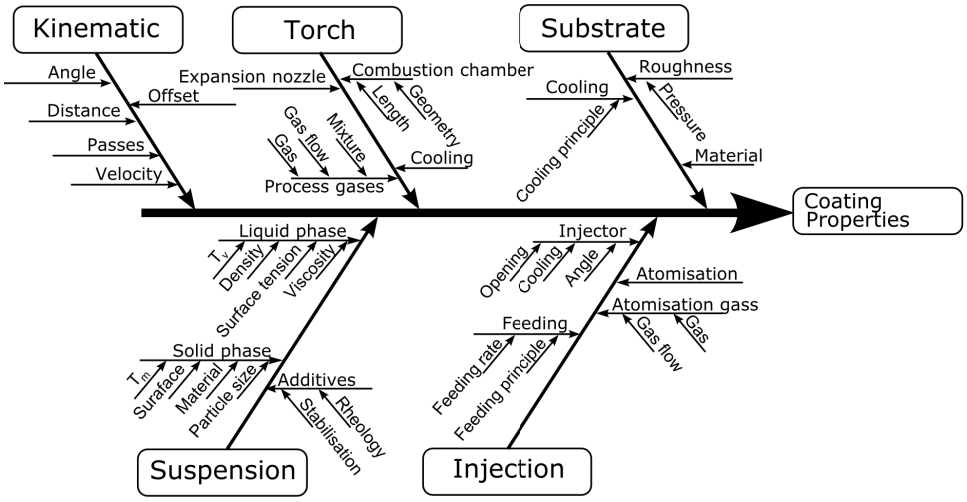

Figure 1: Selection of influencing factors in the HVSFS process.

With all these in place, the case of mixed oxide coatings of alumina and zirconia will be investigated, which have so far been mainly processed via SPS.

Simulation of High Velocity Flame Spraying To gain access to information about the factors leading to the aforementioned process instabilities, a computational fluid dynamic (CFD) modelling approach offers itself as a suitable method. This approach offers insight into factors like local temperatures, gas velocities and flow vectors which directly influence the coating properties via process stability and particle melting behaviour.

The modelling of the numerous thermal spray processes can be approached by different means, as can be seen from literature. This wide variety of approaches led to the decision to investigate in this work the applicability of several approaches for the given system and also their interactions with each other. To gain insight into the processes and conditions inside the combustion chamber and nozzle of an ethene-fueled HVOF torch, the process was modelled with the commercial CFD software ANSYS CFX 16.2. Of interest were especially the combustion process and flow dynamics.

Convergence behaviour of the simulation showed a dependence on the chosen combination of turbulence model (shear-stress-transport [SST] and k-ε) and combustion reaction scheme (one to three reaction steps). While a good convergence could be reached with the SST turbulence model, combining it with more complex reaction schemes lead to instabilities in the simulation. For those, the well established k-ε turbulence model was chosen. The occurring overestimation of combustion temperatures in some reaction schemes can be attributed to the Eddy Dissipation Model, which is well known to overestimate temperatures in fuel gas rich environments assuming a complete combustion. Increasing the complexity

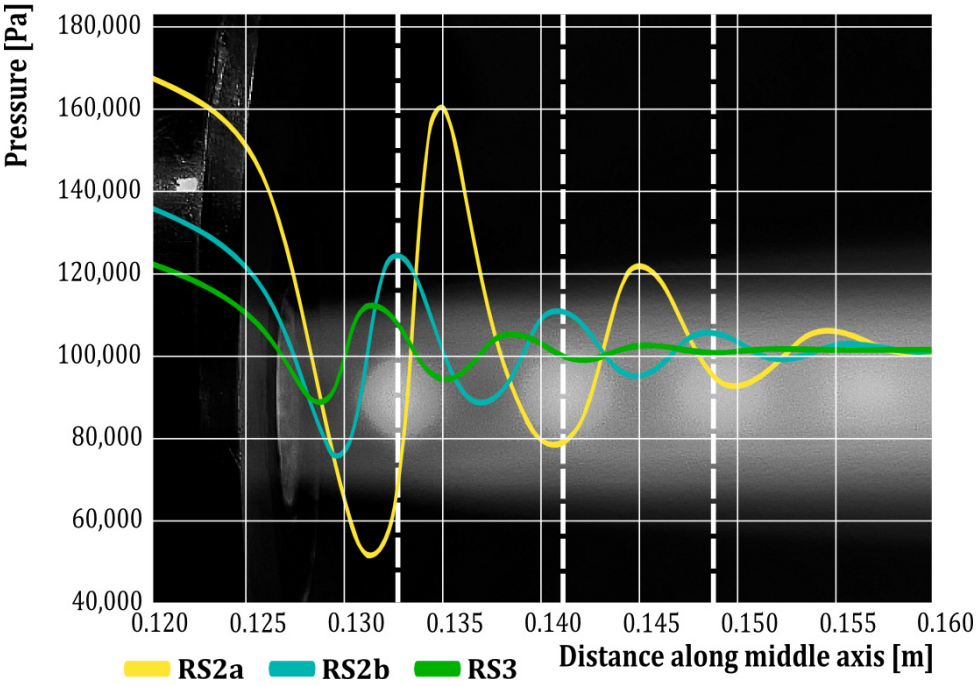

Figure 2: Comparison of the experimentally determined shock diamon position (marked in red) with those determined from local pressures in the different simulation approaches.

of the combustion reaction by adding energy consuming reaction steps lead to a reduction of overall temperatures.

The greatest distances between shock diamonds appeared in two-step-model RS2a, while distances calculated with three-step-model RS3 were the lowest, see Figure 2. Distances derived from reaction scheme RS2b lie between those and show a good match with experimental values. The positions of the shock diamonds also correspond well to the calculated pressures in the combustion chamber. That is, a model with a higher pressure in the combustion chamber also had greater distances between the shock diamonds. Based on the results of the experimental validation, the reaction scheme RS2b in combination with the k- ε -turbulence model was chosen for the investigation of the influence of process parameters and torch components. The optimised two step reaction model RS2b showed a good match with experimental measurements of combustion chamber pressure and shock diamond positions. The geometry of the investigated combustion chambers had a clearly visible effect on the resulting streamlines. The ridge at the outlet of the 19-8-78 combustion chamber resulted in increased turbulent flows. The length of the attached nozzle had no significant influence on the temperatures inside the combustion chamber. A longer nozzle resulted however in a higher gas velocity along the length of the nozzle. A longer nozzle

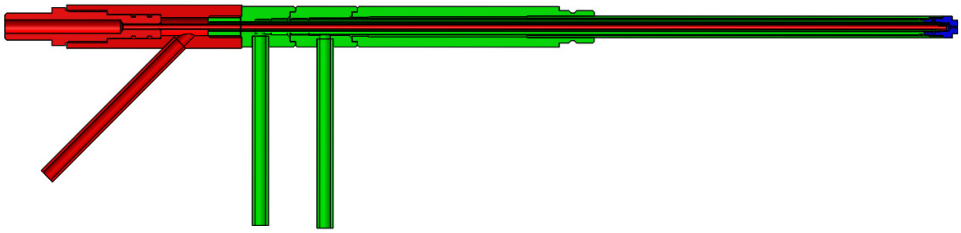

Figure 3: Cross section of the redesigned injector, with the sections of detachable injector nozzle (blue), main body (green) und rear segment with atomisation needle (red).

leads to a longer time of acceleration of the gases. Less turbulence occurred in the longest combustion chamber (30-8-143). Stream lines flowed laminarly along the longer chamber walls in comparison to other geometries. This suggests less deposition of coating material for longer combustion chamber lengths. Less turbulences along the chamber walls lead to higher gas velocities which make it less likely that deposition of coating material occurs. Regarding the absolute pressure, it is notable that it seems independent from the size of the combustion chamber, but to be depending exclusively on the length of the expansion nozzle. The evaluation of the influence of the combustion chamber geometry showed the advantageous nature of longer combustion chambers regarding the deposition of coating material on chamber walls due to reduced turbulence. This is especially the case when considering suspension flame spraying.

Injection Technology While the HVSFS process has established itself as a great potential in manufacturing coatings, the injection of the suspension into the flame is a neuralgic point that poses a great risk for process interruptions due to clogging of the injector. Based on the existing injection technology at the IFKB, developed by Rempp and Schmitt-Radloff, the concept of an internal mixing two fluid nozzle as well as a modular injector design were designed, produced and tested. In general, a two fluid atomization can be seen as an important step towards guaranteeing a stable, robust process. Due to the larger injection diameter and the supporting gas flow of the new concept, the risk of clogging and the unwanted deposition of coating material inside the combustion chamber can be significantly reduced. Also, suspensions with a much higher solid content (up to 40 wt.%) can be processed than with conventional injectors. Due to the resulting higher deposition rate, higher coating thicknesses can be realized in shorter time. Coating quality was also improved due to a reduced number of defects.

The modular approach allows a fast and cheap adaption of the injector to process demands. The injector can be cleaned quickly and the tips can be easily replaced when worn. The thermal insulation reduced the thermal impact on the injector significantly, increasing

process stability and uptime of the injector. In combination with the two fluid nozzle, the use of longer combustion chambers appears beneficial, accomodating the spray cone and the more rapid vaporisation of the fluid. Additionally, three different suspension feeding systems were tested, monitoring feeding behaviour with the help of a pressure sensor. The systems were based on a peristaltic pump, a commercial pressure based system and a newly developed system based on eccentric screw pumps. The displacement pumps showed a strong dependency in their feeding behaviour on the state of wear of the displacement elements. The pressured based system delivered a high consistency with the approbriate sets of parameters, but requires well stabilised suspensions.

Al_2O_3/ZrO_2 Mixed Oxide Coatings The mixed oxide system Al_2O_3/ZrO_2 has in the past mostly been investigated via the SPS process, but is viewed as very promising for application within the HVSFS process. In this work, different approaches to manufacture Al_2O_3/ZrO_2 mixed oxide coatings were investigated. Different compositions Al_2O_3 and ZrO_2 powder feedstocks as well as a commercial pre-alloyed Al_2O_3/ZrO_2 powder feedstock were used and processed with variations in the spraying equipment.

With the application of approbriate additives, beneficial rheological properties and a good stabilisation could be achieved, which permits a stable mass flow in the process and thus consistent coating deposition. Due to few previous experiences with this material system, parameter studies were conducted to find approbriate parameter sets. The main focus was on the best combination of torch components, evaluating different injection concepts in combination with combustion chamber geometries. The combination of the two fluid nozzle with the 30-8-135 combustion chamber was selected as the most advantageous system.

The intermixing of the two phases could be observed in all investigated systems. However, the pre-alloyed powder showed advantages in the even distribution of the phases. In all coatings, ZrO_2-particles can be seen deposited in unmolten and re-solidified state between well-molten splat structures of Al_2O_3 and mixed phases, owing to the higher melting temperature of ZrO_2. All systems showed low porosities. Surface roughness was mostly determined by the particle size of the respective powders, due to their varying Stokes numbers.

In all systems an indentation hardness above 900 HV0,1 could be achieved, the highest values with the fine alumina powder at above 1200 HV0,1. The addition of ZrO_2 lowered the hardness of the coatings. This can possibly attributed to areas of unmolten ZrO_2 agglomerates, deposited between Al_2O_3 splats, as can be seen in figure 4.

Conclusions Understanding the interactions between coating material properties, process parameters and torch and injection equipment is crucial to deliver a stable process and tailor coating properties to respective needs of applications. The new approach of using a

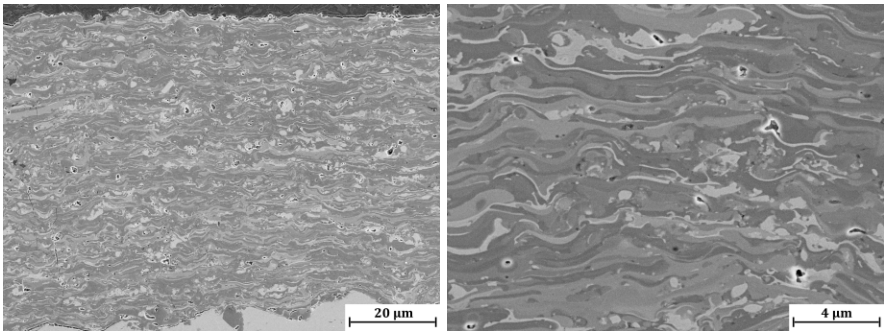

Figure 4: Cross sections of an Al_2O_3/ZrO_2 mixed oxide coating manufactured from prealloyed powder feedstock.

modular, water-cooled suspension injection system with internal gas atomisation has shown much promise in advancing the HVSFS process towards a robust manufacturing system fit for industrial use and allows an advanced adaption of the spraying equipment towards process needs. The supporting gas flow keeps the injection nozzle from clogging up and breaks up powder agglomerates in the suspension, which reduces the deposition of coating materials in the combustion chamber. The critical problem areas of high temperature near the injection point identified in the numerical simulation are thus eliminated. This allowed for Al_2O_3/ZrO_2 mixed oxide coatings to be manufactured with a low defect density and good physical properties.